

# Electronic transport through a double-quantum-dot Aharonov-Bohm interference device with impurities

Wei-Jiang Gong<sup>1,2,\*</sup>, Xue-Feng Xie<sup>1</sup>, Yu Han<sup>3</sup>, and Guo-Zhu Wei<sup>1,2</sup>

1. College of Sciences, Northeastern University, Shenyang 110004, China

2. International Center for Material Physics, Acadmia Sinica, Shenyang 110015, China

3. Physics Department, Liaoning University, Shenyang 110015, China

(Dated: November 8, 2018)

The impurity-related electron transport through a double quantum dot (QD) Aharonov-Bohm (AB) interferometer is theoretically studied, by considering impurities coupled to the QDs in the interferometer arms. When investigating the linear conductance spectra *vs* the impurity levels, we show that the impurities influence the electron transport in a nontrivial way, since their suppressing or enhancing the electron tunneling. A presented single-level impurity leads to the appearance of Fano lineshapes in the conductance spectra in the absence of magnetic flux, with the positions of Fano antiresonances determined by both the impurity-QD couplings and the QD levels separated from the Fermi level, whereas when a magnetic flux is introduced with the the phase factor  $\phi = \pi$  the impurity-driven Breit-Wigner lineshapes appear in the conductance curves. Besides, the nonlocal impurities alter the period of conductance change *vs* the magnetic flux. The multi-level impurities indeed complicate the electron transport, but for the cases of two identical local impurities coupled to the respective QDs with uniform couplings or a nonlocal impurity coupled to both QDs uniformly, the antiresonances are only relevant to the impurity levels. When many-body effect is managed within the second-order approximation, we also find the important role of the Coulomb interaction in modifying the electron transport.

PACS numbers: 73.21.La, 73.63.-b, 73.23.Hk

## I. INTRODUCTION

Current experimental developments and advances at the nanometer scale have allowed to realize and manipulate QDs in a controlled way<sup>1</sup>, which motivated researchers to devote themselves to the electron properties in QD systems with the observation of the atom-like characteristics of a QD, such as the discrete electron level and strong electron correlation<sup>2</sup>, conductance oscillation, and the Kondo effect<sup>3,4,5</sup>. And these features permitted to employ QDs to build various nano-devices, including rectifiers, amplifiers, lasers, etc<sup>6,7,8</sup>.

Due to their similitude with natural atoms, QDs are usually viewed as artificial atoms, and then two or more coupled QDs are regarded as artificial molecules. Multiple QD systems are of particular interest and importance, since they possess higher freedom and admit different kinds of connections to leads in implementing some functions of quantum devices<sup>6,7,8,9,10</sup>. With respect to various multiple-QD structures, the configurations of double QDs, i.e., the simplest coupled QDs, have received more attention than the others both experimentally and theoretically<sup>11</sup>. Initially, most of studies considered serially-coupled double QDs<sup>12</sup>, but posteriorly the T-shaped and parallel configurations were examined<sup>13,14,15,16,17,18,19</sup>, in which the quantum interference are comparatively complicated due to the existence of different transmission paths, and the peculiar electron transport properties in them were thereby found, respectively. It is known that for the structures of T-shaped QDs, when either eigenlevel of the side-coupled QDs reaches the

Fermi level of the system the electron transmission is sharply suppressed which is the so-called antiresonance phenomenon<sup>18</sup>. As for the parallel double-QD configurations, they, also described as the double-QD molecule embedded in an AB ring, have also been extensively investigated, where the presence of a magnetic flux adds a new tool in the control of electron transport behaviors<sup>19,20</sup>. Accordingly, the AB oscillations have been observed theoretically, accompanied by the support of lots of experimental works. Then, the phenomenon of the effective flux-dependent level attraction was also found.<sup>20</sup> On the other hand, in the cases of the appropriate QD-lead couplings, the well-known Fano effect was examined, which motivated many studies about this issue, including the tunable Fano line-shape by the magnetic or electrostatic fields applied on the QDs,<sup>21,22</sup> the Kondo resonance associated Fano effect,<sup>23,24</sup> Coulomb-modification on the Fano effect,<sup>25</sup> the relation between the dephasing time and the Fano parameter  $q$ <sup>26</sup>, and the spin-dependent Fano effect associated with the Rashba spin-orbital (SO) coupling.<sup>27,28</sup>

Despite these mentioned works, so far it is still a formidable challenge to fabricate two clean QDs in the experiments due to irregularities and defects in the QD system. Some localized states often appear in QD systems, which are hybridized with the QD levels. But they are not coupled directly to the leads, which, thereby, are called the impurity states. In some previous literature, the effect of impurities on the electron coherence transmission through the low-dimensional systems has been reported.<sup>29,30,31,32,33,34,35,36,37,38</sup> Some researchers demonstrated the trapping of a conduc-

tion electron between two identical impurities in a quantum wire (or a QD array), as a result, the quantum interference was modified to a great extent and there appear notable phenomena of bound states in continuum.<sup>29,37</sup> Other groups showed that the impurity-driven Fano resonances in quantum wires are sensitively related to the parameters of impurity, such as its strength, position, and lateral extent, which produces substantially different effects on the Fano resonance. Wu *et al.* studied the phonon-assisted electron transmission through a single QD with impurity scattering effects.<sup>30</sup> The results showed that impurity states have weak influence on the suppression of the shot noise. More recently, in a one-dimensional quantum wire side-hybridized with a single-level impurity, the low-temperature properties of interacting electrons were studied.<sup>31</sup> It reported that the hybridization induces a backscattering of electrons in the wire which strongly affects its low-energy properties. Thereby, one can predict that the impurity states play an important role in the quantum transport process.

With respect to such a topic, it is desirable to investigate the influence of impurities on electron transport coupled-QD structures. In the present paper, we study the quantum interference in electron transport through a double QD AB interferometer modified by impurities side-coupled to the QDs in its arms. As a result, it is found the notable contribution of impurities to the electron transmission through this structure. We show that the presence of a single-level impurity induces the appearance of Fano lineshapes in the conductance spectra in the zero-magnetic-field case, whereas it drives the conductance spectra to exhibit Breit-Wigner lineshapes by the presence of magnetic flux, in which the properties of the corresponding lineshapes are strongly determined by the impurity-QD couplings. Besides, the nonlocal impurities alter the period of conductance change *vs* the magnetic flux. The multi-level impurities further transform the electron transport with the complication of conductance curves, but for the cases of each QD couples to the impurities uniformly, the antiresonances are only relevant to the impurity levels. Also, we see the interesting effect of the Coulomb interaction on the adjustment of the electron traveling.

## II. THE THEORETICAL MODEL

The double QD AB interferometer under consideration is schematically illustrated in Fig.1. The system Hamiltonian is written as

$$H_0 = \sum_{\sigma\alpha k \in L,R} \varepsilon_{\alpha k} c_{\alpha k\sigma}^\dagger c_{\alpha k\sigma} + \sum_{\sigma,j=1}^2 \varepsilon_j d_{j\sigma}^\dagger d_{j\sigma} + \sum_{\sigma,\alpha,k,j} V_{j\alpha,\sigma} d_{j\sigma}^\dagger c_{\alpha k\sigma} + \text{H.c.}, \quad (1)$$

where  $c_{\alpha k\sigma}^\dagger$  and  $d_{j\sigma}^\dagger$  ( $c_{\alpha k\sigma}$  and  $d_{j\sigma}$ ) with the spin  $\sigma = \uparrow, \downarrow$  is an operator to create (annihilate) an electron of the state  $|k, \sigma\rangle$  in lead- $\alpha$  ( $\alpha = L, R$ ) and  $|j, \sigma\rangle$  in QD- $j$  ( $j = 1, 2$ ).  $\varepsilon_{\alpha k}$  and  $\varepsilon_j$  are the corresponding single-particle energy.  $V_{j\alpha,\sigma}$  denotes the QD-lead coupling strength. We adopt a uniform QD-lead coupling configuration which gives that  $V_{1L,\sigma} = V_{1R,\sigma}^* = V e^{i(\phi/4 + \sigma\varphi)}$  and  $V_{2R,\sigma} = V_{2L,\sigma}^* = V e^{i\phi/4}$  with the constant  $V$ . The phase shift  $\phi$  is associated with the threaded magnetic flux  $\Phi$  by a relation  $\phi = 2\pi\Phi/\Phi_0$ , in which  $\Phi_0 = h/e$  is the flux quantum. Besides, if the Rashba interaction is applied to either QD, eg., QD-1,  $V_{1\alpha,\sigma}$  will involve the spin-dependent phase  $\sigma\varphi$ , which arises from the electron spin precession induced by the Rashba SO coupling<sup>27,28</sup>.

To study the electronic transport properties, the linear conductance of the noninteracting system at zero temperature is obtained by the Landauer-Büttiker formula<sup>39</sup>

$$\mathcal{G} = \sum_{\sigma} \mathcal{G}_{\sigma} = \frac{e^2}{h} \sum_{\sigma} T_{\sigma}(\omega)|_{\omega=\varepsilon_F}. \quad (2)$$

$T_{\sigma}(\omega)$ , the transmission function, in terms of Green function takes the form as<sup>40</sup>  $T_{\sigma}(\omega) = \text{Tr}[\Gamma_{\sigma}^L G_{\sigma}^r(\omega) \Gamma_{\sigma}^R G_{\sigma}^a(\omega)]$ .  $\Gamma_{\sigma}^{\alpha}$ , a  $2 \times 2$  matrix, is defined as  $[\Gamma^{\alpha}]_{jj',\sigma} = 2\pi V_{j\alpha,\sigma} V_{j'\alpha,\sigma}^* \rho(\omega)$  describing the coupling strength between the QDs and lead- $\alpha$ . We will ignore the  $\omega$ -dependence of  $\Gamma_{jj',\sigma}^{\alpha}$  since the electron density of states in lead- $\alpha$ ,  $\rho(\omega)$ , can be usually viewed as a constant. The retarded and advanced Green functions in Fourier space are involved, which can be solved by means of the nonequilibrium Green function technique and equation-of-motion method.<sup>40,41</sup> By a straightforward derivation, we obtain the retarded Green functions written in a matrix form as

$$G_{\sigma}^r(\omega) = \begin{bmatrix} g_{1\sigma}(z)^{-1} & i\Gamma_{12,\sigma} \\ i\Gamma_{21,\sigma} & g_{2\sigma}(z)^{-1} \end{bmatrix}^{-1}. \quad (3)$$

$g_{j\sigma}(z) = (z - \varepsilon_j + i\Gamma_{jj,\sigma})^{-1}$  with  $z = \omega + i0^+$  and  $\Gamma_{jj',\sigma} = \frac{1}{2}([\Gamma^L]_{jj',\sigma} + [\Gamma^R]_{jj',\sigma})$ . In addition, the advanced Green function can be readily obtained via a relation  $[G_{\sigma}^a(\omega)] = [G_{\sigma}^r(\omega)]^{\dagger}$ . Based on the above derivations, the analytical expression of the linear conductance of  $\sigma$ -spin electron can be written out by taking  $\Gamma = 2\pi V^2 \rho(\omega)$ , i.e.,

$$\mathcal{G}_\sigma = \frac{e^2}{h} \frac{\varepsilon_1^2 + \varepsilon_2^2 + 2\varepsilon_1\varepsilon_2 \cos(\phi + 2\sigma\varphi)}{[\varepsilon_1\varepsilon_2 - \Gamma^2 + \Gamma^2 \cos^2(\frac{\phi}{2} + \sigma\varphi)]^2 + (\varepsilon_1 + \varepsilon_2)^2\Gamma^2} \Gamma^2 \quad (4)$$

### III. NUMERICAL RESULTS AND DISCUSSION

With the formulation developed in the section above, we can carry out the numerical calculation to investigate the linear conductance of this double-QD structure modulated by impurities coupled to QDs. Prior to calculation, we take the strength of the uniform QD-lead couplings  $\Gamma$  as the unit of energy and the Fermi level  $\varepsilon_F$  as the zero point of energy.

To begin with, we do not take the Rashba SO coupling into account (then, the electron transport is independent of the spin index), and for simplicity we focus on the structure of uniform QD levels by letting  $\varepsilon_j = \varepsilon$ . Thereby, in the absence of impurity the electron transport results of this structure are ascertained with the help of Eq.(4): In the zero-external-flux case  $\mathcal{G}$  has a compact expression as  $\frac{2e^2}{h} \frac{4\Gamma^2}{\varepsilon^2 + 4\Gamma^2}$ , the same as the result of the single-channel electron transmission with the QD level  $\varepsilon$  and QD-lead coupling  $2\Gamma$ , whose value is obviously determined by the relative values of QD levels with respect to the Fermi level of this system; however, irrelevant to the shift of QD levels, a threaded magnetic flux with the phase factor  $\phi = \pi$  can lead to the conductance equal to zero.<sup>20</sup>

#### A. Local impurity-QD coupling

For the case where in the interferometer arms there exist impurities coupled to the QDs respectively, i.e., the impurities couple to QDs locally, the Hamiltonian of this system should be rewritten as  $H = H_0 + H_I + H_T$ .  $H_I$  describes electrons in the impurities, which takes a form as

$$H_I = \sum_{m\sigma} (\epsilon_m a_{m\sigma}^\dagger a_{m\sigma} + \chi_m a_{m+1,\sigma}^\dagger a_{m\sigma} + \text{H.c.}) + \sum_{n\sigma} (\epsilon_n b_{n\sigma}^\dagger b_{n\sigma} + \lambda_n b_{n+1,\sigma}^\dagger b_{n\sigma} + \text{H.c.}), \quad (5)$$

with  $a_{m\sigma}^\dagger$  and  $b_{n\sigma}^\dagger$  ( $a_{m\sigma}$  and  $b_{n\sigma}$ ) ( $m, n \geq 1$ ) denoting the creation (annihilation) operator of electron in impurities.  $\epsilon_m$  and  $\epsilon_n$  are the single-energy levels of the corresponding impurities, whereas  $\chi_m$  and  $\lambda_n$  represent the coupling coefficients between two impurities.  $H_T$  describes the electron tunneling between the QDs and impurities

$$H_T = \sum_{\sigma} (t_1 a_{1\sigma}^\dagger d_{1\sigma} + t_2 b_{1\sigma}^\dagger d_{2\sigma} + \text{H.c.}), \quad (6)$$

in which  $t_j$  are the couplings between QDs and impurities. Consequently, in such a case we have

$g_{j\sigma}(z) = (z - \varepsilon_j - \Sigma_{j\sigma} + i\Gamma_{jj,\sigma})^{-1}$ . The selfenergies  $\Sigma_{j\sigma}$ , originating from the couplings of impurities to the QDs of the interferometer, can be written out explicitly as  $\Sigma_{1\sigma} = \frac{t_1^2}{z - \varepsilon_1 - \frac{\chi_1^2}{z - \varepsilon_2 - \dots}}$  and  $\Sigma_{2\sigma} = \frac{t_2^2}{z - \varepsilon_1 - \frac{\lambda_1^2}{z - \varepsilon_2 - \dots}}$ .<sup>42</sup> Therefore, the effect of the local impurities only consists in renormalizing the QD levels as  $\tilde{\varepsilon}_{j\sigma} = \varepsilon_j + \Sigma_{j\sigma}$ .

Then, we concentrate on the characteristics of the linear conductance for the case of a single-level impurity coupled to either QD of the interferometer (e.g., QD-2 here). By taking  $\varepsilon_1 = \varepsilon_0$ ,  $t_2 = \Gamma$ , and  $t_1 = \lambda_1 = 0$ , we show the calculated results of the conductance  $\mathcal{G}$  influenced by the single-level impurity in Fig.2. From Fig.2(a), we can find that when the QD levels are consistent with the Fermi level, the conductance is equal to  $2e^2/h$ , the same as the zero-impurity results. This means that in such a case the impurity cannot affect the quantum transport through the structure. However, a presented magnetic flux changes the role of impurity in this quantum coherent transport process, namely, for the cases of a finite magnetic flux through the interferometer, the profiles of conductance *vs*  $\varepsilon_0$  present Breit-Wigner lineshapes, and also, with the increase of magnetic flux the width of the conductance peak becomes narrow, respectively corresponding to the dotted and dashed lines in Fig.2(a). It is readily found that in the presence of one impurity coupled to QD-2,  $\tilde{\varepsilon}_{2\sigma}$  is expressed as  $\varepsilon - t_2^2/\varepsilon_0$ , so when  $\varepsilon = 0$  the conductance can be simplified as  $\mathcal{G} = \frac{2e^2}{h} \frac{t_2^2}{\varepsilon_0^2(1 - \cos^2(\frac{\phi}{2}))^2 + t_2^2}$ , and it is not difficult to understand the contribution of impurity to the electronic transport under such a condition.

We next focus on the situations of the QD levels separated from the Fermi level of the system (i.e.,  $\varepsilon \neq 0$ ), with the results of  $\varepsilon = 0.5\Gamma$  shown in Fig.2(b). From the figure, one can find that in the absence of magnetic flux, the conductance spectrum shows a Fano lineshape with its antiresonant point around the point of  $\varepsilon_0 = \Gamma$  and the Fano resonance peak in the vicinity of  $\varepsilon_0 = 2\Gamma$ . So, opposite to the  $\varepsilon = 0$  results the effect of impurity here on the quantum transport is more apparent because of the suppression or enhancement of the electron transmission with the change of impurity level. When a magnetic flux is presented with  $\phi = \frac{\pi}{2}$  the conductance profile does not show the Breit-Wigner lineshape any more. Only with the further increase of magnetic flux to  $\phi = \pi$ , the conductance curve, analogous to the results of  $\varepsilon = 0$ , also exhibits a Breit-Wigner lineshape, but its peak departs from

the zero point of energy. Fig.2(c) offers us the conductance results of  $\varepsilon = \Gamma$ , and, it can be seen that different from that in Fig.2(b), when  $\phi = 0$  the Fano lineshape in the conductance spectrum turns to be more clear, and its antiresonance valley emerges in the vicinity of  $\varepsilon_0 = \frac{\Gamma}{2}$  with the resonance peak at the point of  $\varepsilon_0 = \Gamma$ . Alternatively, although in the case of  $\phi = \pi$  the lineshape of conductance curve keeps ‘Breit-Wigner’, its peakwidth is correspondingly narrow and the conductance peak undergoes a further right shift. So far, the contribution of the single-level impurity to the electron transport can be concluded as follows. At the zero-external-field situation, only when the QD levels depart from the Fermi level the impurity can modulate (enhance or weaken) the electron traveling through the structure, since the appearance of Fano lineshape in the conductance spectrum; on the other hand, when there is a threaded magnetic flux with  $\phi = \pi$ , not only the original destructive quantum interference can be changed, but also the resonant tunneling can be realized with the appearance of the Breit-Wigner lineshape in the conductance spectrum, irrelevant to the change of QD levels.

With the help of the results in Fig. 3, this single-level-impurity induced Fano effect can be detailedly analyzed. By virtue of the results in Fig. 3(a) where  $\varepsilon = 0.5\Gamma$ , we can readily find that with the strengthening of the impurity-QD coupling the Fano lineshape in the conductance curve shifts right, followed by the wideness of antiresonance valley proportionally. Via a further observation, we know that the antiresonance position is tightly associated with the impurity-QD coupling strength, and at the point of  $\varepsilon_0 \approx t_2^2$  there occurs Fano antiresonance in electron tunneling through such a system. That is to say, in this configuration the antiresonant point in the conductance spectrum can reflect the coupling strength between the impurity and QD, which may be helpful for the current experiment in the low-dimensional physics. Then, by fixing the QD levels at  $\varepsilon = \Gamma$ , we plot the conductance spectra with the increase of  $t_2$ , as shown in Fig.3(b). Distinctly, although the antiresonance point shifts right with the increment of the QD-impurity coupling, the relation between the antiresonance and the QD-impurity coupling is different from the results in the above case, i.e., here the antiresonant point comes into being at the position of  $\varepsilon_0 \sim \frac{t_2^2}{2}$  in principle. Therefore, it is clear that the presentation of the antiresonance is dependent on both the QD-impurity coupling strength as well as the separation of the QD levels from the Fermi surface.

In order to discuss the impurity-induced Fano resonances we would like to write the conductance expression as its Fano form. Without loss of generality, the Fano form of the conductance formula can

be easily obtained

$$\mathcal{G} = \sum_{\sigma} \frac{e^2}{h} T_{b\sigma} \frac{|e_{\sigma} + q_{\sigma}|^2}{e_{\sigma}^2 + 1}, \quad (7)$$

where  $T_{b\sigma} = \frac{\Gamma_{11,\sigma}^L \Gamma_{11,\sigma}^R}{\Gamma_{11,\sigma}^2}$ ,  $e_{\sigma} = \frac{-\text{Re}G_{22,\sigma}^r / \text{Im}G_{22,\sigma}^r}{\Gamma_{11,\sigma}^L}$ , and  $q_{\sigma} = \frac{-\frac{\tilde{\varepsilon}_{1\sigma}}{\Gamma_{11,\sigma}} (\Gamma_{12,\sigma}^L \Gamma_{21,\sigma}^R \Gamma_{11,\sigma} - T_{b\sigma} \Gamma_{12,\sigma} \Gamma_{21,\sigma} \Gamma_{11,\sigma})}{(\Gamma_{11,\sigma}^L \Gamma_{11,\sigma}^R \Gamma_{22,\sigma} - T_{b\sigma} \Gamma_{12,\sigma} \Gamma_{21,\sigma} \Gamma_{11,\sigma})}$ . Under the condition of uniform QD-lead coupling,  $q_{\sigma}$  can be simplified as  $q_{\sigma} = -\frac{\tilde{\varepsilon}_{1\sigma}}{\Gamma_{11,\sigma}} [e^{i(\phi+2\sigma\varphi)} - T_{b\sigma} \cos^2(\frac{\phi}{2} + \sigma\varphi)] / [1 - T_{b\sigma} \cos^2(\frac{\phi}{2} + \sigma\varphi)]$  and  $e_{\sigma} = -\frac{\tilde{\varepsilon}_{2\sigma}}{\Gamma_{11,\sigma}} [1 + T_{b\sigma} \cos^2(\frac{\phi}{2} + \sigma\varphi) \frac{\tilde{\varepsilon}_{1\sigma}}{\tilde{\varepsilon}_{2\sigma}}] / [1 - T_{b\sigma} \cos^2(\frac{\phi}{2} + \sigma\varphi)]$ . It is seen that, for the case shown in Fig.2(a) in which the Rashba interaction is absent and the uniform QD levels coincide with the Fermi level,  $q_{\sigma}$  is equal to zero, so the conductance profile does not exhibit the Fano lineshape. Concretely, when  $\phi = 0$   $e_{\sigma}$  gets close to infinity all long, which induces the result of  $\mathcal{G} \equiv 2e^2/h$ . With regard to the results shown in Fig.2(b)-(c), in the zero-magnetic-field case the separation of  $\varepsilon$  from the Fermi level makes  $q_{\sigma}$  nonzero and  $e_{\sigma}$  convergent, thereby, the Fano lineshape comes about in the conductance spectrum. Moreover, the antiresonant points in the conductance spectra can be ascertained by considering  $e_{\sigma} + q_{\sigma} = 0$ . Via a simple derivation, the position of antiresonance can be obtained analytically, when  $\varepsilon_0 = \frac{t_2^2}{2\varepsilon}$  the conductance encounters zero which means the occurrence of the antiresonance effect. Based on this result, one can understand the quantitative dependence of the antiresonance point on both the strength of impurity-QD coupling and the values of QD levels. Therefore, in such a structure, the occurrence of Fano antiresonance remarkably differs from those in the single-channel system with impurity, where the antiresonance occurs once the impurity level is aligned with the Fermi level<sup>18</sup>. The position of Fano peak can be obtained as well, accordingly, just at the point of  $\frac{t_2^2}{\varepsilon}$  there emerges the Fano resonance. Meanwhile, it is certain that changing the position of QD levels with respect to the Fermi level can lead to the variation of the sign of  $\varepsilon$ , then, the sign of  $q_{\sigma}$  alters which brings out the inversion of the Fano lineshape, corresponding to the shot-dashed line in Fig.3. Up to now, in this structure the Fano effect driven by a single-level impurity has been clarified.

According to the results in Fig.2, when  $\phi = \pi$   $q_{\sigma} = \frac{\tilde{\varepsilon}_{1\sigma}}{\Gamma_{11,\sigma}}$  is real, but the conductance curves present Breit-Wigner lineshapes, independent of the deviation of QD levels from the Fermi level. The only phenomenon is that with the increase of  $\varepsilon$ , the conductance peak becomes narrow following its right shift. Thus, such results do not coincide with the previous discussions that only an imaginary  $q_{\sigma}$  could cause the appearance of a Breit-Wigner lineshape in the corresponding conductance.<sup>43</sup> We have to continue to study the behaviors of  $e_{\sigma} + q_{\sigma}$  when  $\phi = \pi$ .

Then, we find that in such a case  $e_\sigma + q_\sigma = \frac{t_2^2}{\Gamma_{\varepsilon_0}}$  has no opportunity to be zero, irrelevant to the QD levels in the quantum transport regime. By a simplification, the conductance can be written explicitly as  $\mathcal{G} = \frac{2e^2}{h} T_{b\sigma} t_2^4 / [(\varepsilon_0 - \frac{\varepsilon t_2^2}{\varepsilon^2 + \Gamma^2})^2 + \frac{\Gamma^2 t_2^4}{\varepsilon^2 + \Gamma^2}]$ . Based on such a result, the exhibition and properties of the Breit-Wigner lineshape in the conductance curve can be well understood, i.e., decreasing the QD-impurity coupling or increasing the value of QD levels can lead to the narrowness of the conductance peak. Well, in the case of  $\varepsilon = \Gamma$ , the quantities  $\frac{\varepsilon t_2^2}{\varepsilon^2 + \Gamma^2} = \frac{t_2^2}{2\varepsilon}$ , which leads to the superposition of the antiresonant point in the  $\phi = 0$  conductance spectrum and the conductance peak of  $\phi = \pi$ . In addition, all the results above tell us that the magnetic-induced inversion of Fano lineshapes is unfeasible in this model.

Although the above analysis is helpful for understanding the properties of the impurity-driven electron transport, one has to know that the underlying physics in the electron motion of such a structure should be quantum interference, which can be described by means of the language of Feynman path<sup>43</sup>. To illustrate this issue, we rewrite the electron transmission function

$$\text{as } T_\sigma(\omega) = \text{Tr}[\Gamma_\sigma^L G_\sigma^r \Gamma_\sigma^R G_\sigma^a] = \left| \sum_{j,l=1}^2 t_\sigma(j,l) \right|^2,$$

where the electron transmission coefficients are defined as  $t(j,l) = \bar{V}_{Lj,\sigma} G_{jl,\sigma}^r \bar{V}_{lR,\sigma}$  with  $\bar{V}_{j\alpha,\sigma} = \bar{V}_{\alpha j,\sigma}^* = V_{j\alpha,\sigma} \sqrt{2\pi\rho(\omega)}$ . Besides, it is necessary to define  $\tilde{V}_{j\alpha,\sigma} = \tilde{V}_{\alpha j,\sigma}^* = V_{j\alpha,\sigma} \sqrt{\pi\rho(\omega)}$  for the following discussion. At the beginning, we expand the Green function into an infinite geometric series. Taking  $G_{11}^r$  as an example, we have  $G_{11,\sigma}^r = g_{2\sigma}^{-1} / [g_{1\sigma}^{-1} g_{2\sigma}^{-1} + \Gamma_{12,\sigma} \Gamma_{21,\sigma}] = \sum_{j=0}^{\infty} g_{1\sigma} (-g_{1\sigma} g_{2\sigma} \Gamma_{12,\sigma} \Gamma_{21,\sigma})^j$ . Thereby, we can express the transmission coefficient  $t_\sigma(1,1)$  as a summation of Feynman paths with different orders, i.e.,

$$t_\sigma(1,1) = \sum_{j=0}^{\infty} \bar{V}_{L1,\sigma} g_{1\sigma} (-g_{1\sigma} g_{2\sigma} \Gamma_{12,\sigma} \Gamma_{21,\sigma})^j \bar{V}_{1R,\sigma} =$$

$$\sum_{j=0}^{\infty} t_{j\sigma}(1,1). \quad \text{By the same token, we can}$$

expand other transmission coefficients as a summation of Feynman paths:

$$t_\sigma(2,2) = \sum_{j=0}^{\infty} \bar{V}_{L2,\sigma} g_{2\sigma} (-g_{2\sigma} g_{1\sigma} \Gamma_{12,\sigma} \Gamma_{21,\sigma})^j \bar{V}_{2R,\sigma} =$$

$$\sum_{j=0}^{\infty} t_{j\sigma}(2,2), \quad t_\sigma(1,2) =$$

$$\sum_{j=1}^{\infty} i \bar{V}_{L1,\sigma} (-g_{1\sigma} g_{2\sigma} \Gamma_{12,\sigma})^j \Gamma_{21,\sigma}^{j-1} \bar{V}_{2R,\sigma} =$$

$$\sum_{j=1}^{\infty} t_{j\sigma}(1,2), \quad \text{and} \quad t_\sigma(2,1) =$$

$$\sum_{j=1}^{\infty} i \bar{V}_{L2,\sigma} (-g_{1\sigma} g_{2\sigma} \Gamma_{21,\sigma})^j \Gamma_{12,\sigma}^{j-1} \bar{V}_{1R,\sigma} = \sum_{j=1}^{\infty} t_{j\sigma}(2,1).$$

With the above analysis, we find that quantum interference occurs among infinite Feynman paths, and only for the case of  $\phi = \pi$  all the higher-order

paths vanish because of the destructive interference among them and the two zero-order paths [ $t_{0\sigma}(1,1)$  and  $t_{0\sigma}(2,2)$ ] remain. We then analyze the respective contributions of the leading Feynman paths to the quantum interference, as shown in Fig.4. From the figure, it is found that  $t_{0\sigma}(1,1)$  provides a nonresonant path for the electron transmission. But, in the other interferometer arm, the coupling between the impurity and QD-2 modulates the feature of  $|t_{0\sigma}(2,2)|^2$  nontrivially because it presents an antisymmetric lineshape with the shift of  $\varepsilon_0$ . Of course, the phase of  $t_{0\sigma}(2,2)$  can also be tuned with the shift of the impurity level. As a result, the interference between these two paths induces the antisymmetric lineshape of the contribution to the conductance in spite of its being greater than unity. When the contribution of the first-order paths is taken into account, the contribution of low-order paths to conductance gets close to the curve of the standard conductance. With this, the occurrence of Fano interference in this system can be well clarified, i.e., just the existence of impurity modifies the phase of electron waves through QD-2 of the interferometer. On the other hand, in the presence of magnetic flux  $\phi = \pi$ , the high-order modification can be safely ignored due to the destructive interference of high-order Feynman paths, and the interference between the two paths gives rise to the appearance of Breit-Wigner lineshape in the conductance spectrum, as shown in Fig.4(b).

With regard to the situation where in both arms there exist impurities, we first would like to consider the simple case that there is a single-level impurity respectively side-coupled to each QD of the interferometer. The corresponding results are shown in Fig.5 in which  $\varepsilon_1 = e_1 = \varepsilon_0$  and  $\chi_1 = \lambda_1 = 0$ . Here, by fixing  $t_2$  at  $\Gamma$  and increasing the amplitude of  $t_1$ , the interplay between the impurities in the two arms on the quantum interference is easy to be understood. Just in Fig.5(a), we can see that the nonzero  $t_1$  changes the electronic transport strikingly with its complicating the original Fano interference, even if a weak coupling between the impurity and QD-1 is considered. To be concrete, in the case of zero magnetic flux, except the antiresonance point at the position of  $\varepsilon_0 = \frac{t_2^2}{2\varepsilon}$  the other antiresonance occurs in the vicinity of  $\varepsilon_0 = 0$ . By virtue of the results in previous works, this phenomenon can be explained as follows. In the presence of an impurity side-coupled to one QD, the electron transport in the corresponding channel will be suppressed completely when the impurity is aligned with the Fermi level<sup>18</sup>. Thus, when both the impurity levels are identical with the Fermi level, the electron transmission in both channels of the interferometer are restrained, which, independent of the application of magnetic flux, results in the appearance of antiresonance at the point of  $\varepsilon_0 = 0$ . So, when  $\phi = \pi$ , there is also a Fano antiresonance in the conductance spectrum at the point of  $\varepsilon_0 = 0$ . In addition, with the increment of  $t_1$

from  $0.2\Gamma$  to  $\Gamma$ , the original Fano antiresonance ( at the point of  $\varepsilon_0 = \frac{t_2^2}{2\varepsilon}$  ) shifts right and the antiresonance valley becomes narrow until its disappearance, but, the antiresonant point at the Fermi level is fixed and the corresponding antiresonance valley widens. This is for reason that the increase of  $t_1$  the property of  $g_{1\sigma}$  gets close to that of  $g_{2\sigma}$ , and, just when  $t_1 = t_2$   $g_{1\sigma}$  has the same properties as  $g_{2\sigma}$ , which drives the present electron transport similar to that in the single-channel case (i.e., the T-shaped double QDs ). Then, one can readily understand the emergence of conductance zero at the position of  $\varepsilon = 0$  in the zero-magnetic-flux case, as shown in Fig.5(d).

There is no doubt that the consideration of multi-level impurities can further influence the quantum interference in this structure. As shown in Fig.6, we plot the conductance spectra in the case of double-level impurities considered. We can find, from Fig.6(a) with  $\varepsilon = \Gamma$  and  $t_1 = \lambda_2 = 0$ , that when only one double-level impurity is presented in either arm of the interferometer, in the case of zero magnetic flux there are two Fano lineshape existing in the conductance spectrum, the space of which is consistent with the impurity-level space. Similar to those in the case of single-level impurity, the Fano antiresonant points in conductance spectrum of  $\phi = 0$  corresponding to the conductance peak in the case of  $\phi = \pi$ . But, here between the  $\phi = \pi$  conductance peaks an antiresonance comes into being, which can be clarified by paying attention to the interference between  $t_{0\sigma}(1,1)$  and  $t_{0\sigma}(2,2)$ , described by the inset of Fig.6(a). For the case where in each arm there is a double-level impurity, the lineshapes of the conductance become more complex, as shown in Fig.6(b)-(d). In such a case, we fix the values of  $t_2$  and  $\lambda_1$ , while change the amplitudes of  $t_1$  and  $\chi_1$  to analyze the variation of conductance by the two double-level impurities. Surely, both the impurities in different channels contribute to the antiresonances in the  $\phi = 0$  conductance curve and resonances in  $\phi = \pi$  conductance profiles, respectively. It is seen that when  $\phi = \pi$ , compared with the results of one impurity, the antiresonance in the vicinity of Fermi level becomes an insulating band and it is more clear with the increase of  $t_1$ , which also arises from the similar properties of  $g_{1\sigma}$  and  $g_{2\sigma}$ . Similar to the results in Fig.5(d), when the identical impurities respectively couple to the QDs with uniform couplings, the Fano antiresonance is only relevant to the eigenlevels of the impurities (  $\varepsilon_0 \pm \lambda_1$  here ).

As for the extreme case where the levels of impurities become continuous, by assuming  $\epsilon_m = e_n = \varepsilon_0$  and  $t_j = \chi_m = \lambda_n = \Gamma$  we can obtain  $\Sigma_{1(2)\sigma} = \frac{1}{2}(-\varepsilon_0 - i\sqrt{4\Gamma^2 - \varepsilon_0^2})$  in such a case. Under the condition of  $|\varepsilon_0| < 2\Gamma$ ,  $\text{Im}\Sigma_{1(2)\sigma} \neq 0$ . So it can be anticipated that in electron transport through the QDs, there will occur the notable inelastic scattering. As shown in Fig.7(a), even if only there exist continuous-level impurity in one arm of the interfer-

ometer, the electron coherent tunneling through the corresponding channel is seriously restraint. Only at the upper edge of the energy band the Fano interference emerges in the absence of magnetic flux, which is due to that  $\text{Im}\Sigma_{1(2)\sigma} \rightarrow 0$  in this region and then the role of impurity is similar to that of single-level one. However, in Fig.7(b) it is seen that the appearance of an additional concrete-level impurity in the other interferometer arm can enhance the electronic transport. When there exist continuous-level impurities coupled to both the QDs, no Fano lineshape comes about in the conductance spectrum any more.

Next, we have to make a remark regarding the many-body effect which we have by far ignored. As is known, the many-body effect is an important origin for the peculiar transport properties in QDs. Usually, the many-body effect is incorporated by considering only the intradot Coulomb repulsion, i.e., the Hubbard term. If the Hubbard interaction is not very strong, we can truncate the equations of motion of the Green functions to the second order. By a straightforward derivation, we find that in such an approximation, only the relevant QD and impurity levels are renormalized, i.e.,  $\varepsilon_{j\sigma} = \varepsilon_j \left( \frac{z - \varepsilon_j - U_j}{z - \varepsilon_j - U_j + U_j \langle n_{j\sigma} \rangle} \right)$ ,  $\epsilon_{m\sigma} = \epsilon_m \left( \frac{z - \epsilon_m - U_m}{z - \epsilon_m - U_m + U_m \langle n_{m\sigma} \rangle} \right)$ , and  $e_{n\sigma} = e_n \left( \frac{z - e_n - U_n}{z - e_n - U_n + U_n \langle n_{n\sigma} \rangle} \right)$ , correspondingly, the formula Eq.(2) is still feasible to calculate the linear conductance.<sup>40,42</sup> As a typical case, in Fig.8, by taking the many-body terms into account, we investigate the linear conductance modified by a single-level impurity, with the structure parameters the same as those in Fig.2(c). From the figure, we can find that when the uniform many-body strength is considered, the conductance spectra are divided into two groups, since the energy level  $\varepsilon_j$  (  $\epsilon_m$  or  $e_n$  ) splits into two, i.e.,  $\varepsilon_j$  and  $\varepsilon_j + U$  (  $\epsilon_m$  and  $\epsilon_m + U$ , or  $e_n$  and  $e_n + U$  ). It is seen that only in the case of  $\varepsilon = \Gamma$  the conductance lineshape in each group keeps the electron transport properties of the non-interacting case. But when  $\varepsilon = -\Gamma$ , the effect of the electron interaction on the electron transport is more remarkable and the lineshapes of the conductance spectra in each group are tightly influenced by the Coulomb strength, as shown in Fig.8(b)-(c), which presents as the disappearance or inversion of the Fano lineshapes caused by the different-strength Coulomb interactions. Such results are due to that the Coulomb repulsion brings about the change of  $q_\sigma$ 's sign ( + or - ). When the appropriate electron interaction in QD-1 is considered, the renormalized level  $\varepsilon_{1\sigma}$  is written as  $\varepsilon_{1\sigma} \left( \frac{z - \varepsilon_{1\sigma} - U_1}{z - \varepsilon_{1\sigma} - U_1 + U_1 \langle n_{1\sigma} \rangle} \right)$ , so, the signs of both  $\varepsilon_{1\sigma}$  and the Fano parameter  $q_\sigma$  ( here  $q_\sigma = -\varepsilon_{1\sigma}/\Gamma$  ) is obviously dependent on the Coulomb strength  $U_1$ .

## B. Nonlocal impurity-QD coupling

With respect to the case of the impurity coupled to both QDs nonlocally, the Hamiltonian  $H_I$  and  $H_T$  should be respectively expressed as

$$H_I = \sum_{\sigma,m} \epsilon_m a_{m\sigma}^\dagger a_{m\sigma} + \sum_{\sigma,m=1}^{N-1} \chi_m a_{m+1,\sigma}^\dagger a_{m\sigma} + \text{H.c.} \quad (8)$$

and

$$H_T = \sum_{\sigma} (t_1 a_{1\sigma}^\dagger d_{1\sigma} + t_2 a_{N\sigma}^\dagger d_{2\sigma} + \text{H.c.}) \quad (9)$$

For simplicity, by means of the theory in Ref.44 we can work out the Green functions involved so as to the conductance.

Then, in Fig.9 the situation of a single-level impurity is first discussed, and by fixing  $t_2$  at  $\Gamma$  we investigate the influence of the presence of  $t_1$  on the conductance properties. From this figure it can be found that when no magnetic flux is taken into account, similar to the results in Fig.3, only in the cases of QD levels separated from the Fermi level there emerge the Fano lineshapes in the corresponding conductance spectra and the excess of QD levels to the Fermi level gives rise to the inversion of the Fano lineshapes. However, the appearance of nonzero  $t_1$  shifts the antiresonance position in the conductance curve to a great extent. First, the antiresonance does not appear at the point of  $\varepsilon_0 = \frac{t_2^2}{2\varepsilon}$  any more but with the increase of  $t_1$  it gets close to the zero point of energy, followed by the widening of the antiresonance valley. Just when  $t_1 = t_2 = \Gamma$  the antiresonance occurs at the point of  $\varepsilon_0 = 0$ , as shown in Fig.9(b)-(c). Besides, it is of importance that the simultaneous couplings of the impurity to QDs alter the period of conductance change ( *vs* magnetic flux ) from  $2\pi$  to  $4\pi$ . Concretely, when the magnetic flux increases to  $\phi = 2\pi$ , the conductances present much differences from those in the zero-magnetic-flux case, as shown in Fig.9(e)-(f), i.e., in such a case the increase of  $t_1$  induces the shift of antiresonance point to the high-energy direction with the narrowness of the antiresonance valley, until the disappearance of antiresonance when  $t_1 = \Gamma$  in which the conductance becomes irrelevant to the tuning of  $\varepsilon_0$ .

Analogous to the discussion in the above subsection, for convenience of analyzing the Fano antiresonance effect here we also rewrite the conductance expression into its Fano form. First, the retarded Green functions that describe the electron motion can be written in a matrix form as

$$G_{\sigma}^r(\omega) = g_{\sigma}(z)^{-1} \cdot \begin{bmatrix} \tilde{g}_{1\sigma}(z)^{-1} & i\tilde{\Gamma}_{12,\sigma} \\ i\tilde{\Gamma}_{21,\sigma} & \tilde{g}_{2\sigma}(z)^{-1} \end{bmatrix}^{-1} \quad (10)$$

where  $\tilde{g}_{j\sigma}(z)^{-1} = g_{j\sigma}(z)^{-1}g_{\sigma}(z)^{-1} - |t_j|^2$ ,  $\tilde{\Gamma}_{12,\sigma} = it_1t_2 + \Gamma_{12,\sigma}g_{\sigma}(z)^{-1}$ , and  $\tilde{\Gamma}_{21,\sigma} = it_1^*t_2^* + \Gamma_{21,\sigma}g_{\sigma}(z)^{-1}$ , with  $g_{\sigma}(z) = [z - \varepsilon_0]^{-1}$  being the impurity Green function in the absence of impurity-QD couplings. Consequently, by letting  $T_{b\sigma} =$

$\Gamma_{11,\sigma}^L \Gamma_{11,\sigma}^R / [\tilde{\varepsilon}_1^2 + \Gamma_{11,\sigma}^2]$  ( with  $\tilde{\varepsilon}_j = \varepsilon_j + |t_j|^2 g_{\sigma}$  ) and  $e_{\sigma} = -\text{Re}G_{22,\sigma}^r / \text{Im}G_{22,\sigma}^r$  the Fano form of the conductance formula can be obtained

$$\mathcal{G} = \sum_{\sigma} \frac{e^2}{h} T_{b\sigma} \frac{|e_{\sigma} + \tilde{q}_{\sigma}|^2}{e_{\sigma}^2 + 1}, \quad (11)$$

and the new Fano parameter is defined as  $\tilde{q}_{\sigma} = -\frac{\tilde{\varepsilon}_1}{\Gamma} [e^{i(\phi+2\sigma\varphi)} - \mathcal{A}_{\sigma} T_{b\sigma}] / [1 - T_{b\sigma}(\mathcal{A}_{\sigma} + \mathcal{B}_{\sigma} \tilde{\varepsilon}_1)]$ , with  $\mathcal{A}_{\sigma} = (\Gamma_{12,\sigma} \Gamma_{21,\sigma} - |t_1 t_2|^2 g_{\sigma}^2) / \Gamma^2$  and  $\mathcal{B}_{\sigma} = (t_1 t_2 \Gamma_{12,\sigma} + t_1^* t_2^* \Gamma_{21,\sigma}) g_{\sigma} / \Gamma^3$ . Then, with the help of the results above, the Fano antiresonance point can be clarified, i.e., at the point of  $\varepsilon_0 = \frac{|t_1 - t_2|^2}{2\varepsilon}$  the conductance becomes zero in the absence of magnetic flux. However, when  $\phi = 2\pi$  the antiresonance point comes into being at the position of  $\varepsilon_0 = \frac{|t_1 + t_2|^2}{2\varepsilon}$ , except for the case of  $t_1 = t_2$  where  $\mathcal{G} \sim \frac{4\Gamma^2}{\varepsilon^2 + 4\Gamma^2}$  is extremely simplified and independent of  $\varepsilon_0$ . On the other hand, notice that the quantum interference in this structure is completely different from the system in the above subsection, and it seems that the quantum interference of this case is relatively complicated since the nonlocal couplings of the impurity to QDs provides an additional channel for the electron transmission. In order to analyze the quantum interference in such a situation, one has to deal with this model in the molecular-orbital representation, because the coupled structure formed by the impurity and QDs can be viewed as a new QD molecule, and just the quantum interference among its eigenstates causes the present conductance results. The detailed demonstration in Ref.44 can help us clarify the picture of quantum interference here.

We next show the conductance spectra in the case of the magnetic flux phase factor  $\phi = \pi$ . It is clear that the conductance spectra always exhibit Breit-Wigner lineshapes, independent of the change of  $t_1$  and  $\varepsilon$ . But, the effect of the nonzero  $t_1$  on the modulation of conductance lineshape can not be ignored. As presented by Fig.10(a) when the QD levels are the same as the Fermi level, i.e.,  $\varepsilon = 0$ , the increment of  $t_1$  causes the widening of the conductance peak. In addition, the results in Fig.10(b)-(c) suggest that for the case of the finite-value QD levels, with the increase of  $t_1$  the conductance peak shifts right as well, accompanied by its widening. When paying attention to the Fano form of the conductance in Eq.(11), we find that there is no probability for  $e_{\sigma} + \tilde{q}_{\sigma}$  to be equal to zero, but the conductance expression can be written as  $\mathcal{G} = \frac{2e^2}{h} T_{b\sigma} (t_1^2 + t_2^2)^2 / [(\varepsilon_0 - \frac{\varepsilon(t_1^2 + t_2^2)}{\varepsilon^2 + \Gamma^2})^2 + \frac{\Gamma^2(t_1^2 + t_2^2)^2}{\varepsilon^2 + \Gamma^2}]$ , by which the conductance properties in this case can be well understood.

When there is a nonlocal double-level impurity coupled to the QDs, from Fig.11 where the conductances of  $\phi = 0$  and  $\phi = 2\pi$  are discussed, we can find that the role of the impurity in changing the quantum transport is also remarkable in comparison with the results of  $t_1 = 0$  in Fig.6(a). Just as exhibited in Fig.11(a) and (d), in this case even if

$\varepsilon$  is set to be zero, the extra coupling between the impurity and QD-1 leads to the occurrence of antiresonance: For the zero-magnetic-flux case by the increase of  $t_1$  to  $t_1 = \Gamma$  the antiresonance position shifts left to  $\varepsilon_0 = -\Gamma$  but when  $\phi = 2\pi$  the antiresonant point shifts right to  $\varepsilon_0 = \Gamma$  following the wideness of the antiresonance valley. When the QD levels are separated from the Fermi level with  $\varepsilon = 0.5\Gamma$  in Fig.11(b) and (e) or  $\varepsilon = \Gamma$  in Fig.11(c) and (f), taking the case of  $t_1 = 0.1\Gamma$  as an example, the contribution of  $t_1$  to the conductance is obvious since the differences between the conductance of  $\phi = 0$  and  $\phi = 2\pi$ . Namely, in the low or high energy regimes, the widths of the antiresonance valleys when  $\phi = 0$  are different from those in the case of  $\phi = 2\pi$ , respectively; in addition, when  $\phi = 2\pi$  the space between the two antiresonant points is smaller compared with the results in the case of  $\phi = 0$ . Furthermore, with the increase of  $t_1$ , in the absence of magnetic flux the antiresonance point in the high-energy regime goes to vanish and the antiresonance appears at the position of  $\varepsilon_0 = -\Gamma$ , whereas in the case of  $\phi = 2\pi$  antiresonance in the low-energy regime disappears and the antiresonance holds at the point of  $\varepsilon_0 = \Gamma$ . Therefore, it can be concluded that independent of the QD levels, when the double-level impurity couples to both QDs uniformly, the conductance zero is associated with the antibonding state of the impurity when  $\phi = 0$  but when the magnetic phase factor is tuned to  $\phi = 2\pi$  the conductance zero emerges in the case of the bonding state of impurity identical with the Fermi level.

Finally, with respect to the case of the magnetic flux phase factor  $\phi = \pi$ , via the results in Fig.12(a)-(c) it is found that despite the nonzero  $t_1$  the appearance of double-level impurity also gives rise to two resonant peaks in the conductance spectra, while in this case no antiresonance comes about between the two conductance peaks, but the increase of  $t_1$  can efficiently elevate the conductance valley. Combining with the above results, we can further understand the influence of finite-value  $t_1$  on the quantum interference in this structure. When a triple-level impurity is considered, as shown in Fig.12(d), the effect of nonlocal multi-level impurity can be completely uncovered. It can be anticipated that under the condition of the uniform couplings of multi-level nonlocal impurity to both QDs, when  $\phi = 0$  the conductance zeros are associated with the odd-numbered (even-numbered) eigenlevels of the odd-level (even-level) impurity but when  $\phi = 2\pi$  the opposite phenomenon will come into being.<sup>44</sup>

With regard to the many-body effect in such a case of nonlocal impurity, we take the example of single-level impurity to show the change of conductance spectra. From Fig.13 with the identical QD-impurity couplings, we can find that when Coulomb repulsions are sufficiently strong, analogous to the results of local impurity, the spectra have the opportunity to be divided into two groups. And also, in

the cases of  $\varepsilon = -\Gamma$  the electron interactions present remarkable effect on the electron transport. However, in such a case the Coulomb interactions do not lead to the disappearance or inversion of the Fano lineshapes. By employing the results of Eq.(11), one can understand this phenomenon. It is of course that under the condition of the nonlocal couplings, the Fano parameter  $q_\sigma$  are modulated by the impurity level as well, then, mathematically the presence of Coulomb interactions influences the signs and values of the levels of QDs and impurity ( $\varepsilon_1$  and  $\epsilon_1$ ), which weakens the effect of Coulomb interactions on the Fano parameter.

#### IV. SUMMARY

In conclusion, in this paper we have theoretically investigated the quantitative effect of the local and nonlocal impurities on the electron transport through a double-QD AB interferometer, by assuming impurities to couple to the QDs in the interferometer arms. By plotting the linear conductance spectra *vs* the impurity levels, we have found that at the zero-magnetic-flux case, the conductance spectra show up as the Fano lineshapes even if the presence of a single-level impurity, but the impurity-caused Breit-Wigner lineshapes emerge in the conductance spectra when the magnetic flux phase factor  $\phi = \pi$ . Besides, the nonlocal coupling of impurities to the QDs changes the period of conductance change *vs* the magnetic flux from  $2\pi$  to  $4\pi$ . These indicate the nontrivial influence of impurities on the electron transport in this system. Furthermore, it has been seen that for the cases of two identical impurities respectively coupled to the QDs with uniform couplings or an impurity coupled to both QDs uniformly, the Fano antiresonances are only relevant to the impurity levels, including the more interesting transmission behaviors at the nonlocal-impurity cases. By considering the many-body effect within the second-order approximation, we also found the important role of the Coulomb interaction in such an electron transport process. All these results are analyzed in detail, and we expect that the discussion in such a work can be helpful for the relevant experiment.

In the end, we would like to discuss the impurity-driven spin-dependent electron transport when the Rashba interaction is taken into account. Based on the theoretical description, when the Rashba interaction is applied to the vicinity of either QD, e.g., QD-1, there will be a spin-dependent phase factor  $\sigma\varphi$  added to the QD-lead coupling coefficients  $V_{1\alpha,\sigma}$ , then, the interplay of the magnetic and Rashba fields makes the conductance spectra of the opposite-spin electron separated from each other<sup>27,28</sup>. Typically, when the strengths of these two fields are assumed to be  $\phi = \frac{\pi}{2}$  and  $\varphi = \frac{\pi}{4}$ , respectively, the up-spin electron thereby undergoes a  $\pi$ -phase-factor quan-

tum interference while the down-spin electron undergoes a zero-phase-factor quantum interference, so the apparent spin polarization occurs in the electron transport process. Of course, the impurity can not contribute to the occurrence of spin polarization. Here, we readily emphasize that in the cases of

different-property interferences, the impurity plays different roles, i.e., the suppressing or enhancement of electron transmission, so the impurity can efficiently invert the spin polarization when the Rashba interaction is introduced, and such an effect will be more clear when multi-level impurity is considered.

---

\* Email address: weijianguong@gmail.com

- <sup>1</sup> J. R. Petta, A. C. Johnson, J. M. Taylor, E. A. Laird, A. Yacoby, M. D. Lukin, C. M. Marcus, M. P. Hanson, and A. C. Gossard, *Science* **309**, 2180 (2005); A. K. Hüttel, S. Ludwig, H. Lorenz, K. Eberl, and J. P. Kotthaus, *Phys. Rev. B* **72**, 081310(R) (2005).
- <sup>2</sup> L. P. Kouwenhoven, N. C. van der Vaar, A. T. Johnson, W. Kool, C. J. P. M. Harmans, J. G. Williamson, A. A. M. Staing, and C. T. Foxon, *Z. Phys. B: Condens. Matter* **85**, 367 (1991).
- <sup>3</sup> D. Goldhaber-Gordon, H. Shtrikman, D. Mahalu, D. A. Magder, U. Meirav, and M. A. Kastner, *Nature (London)* **391**, 156 (1998).
- <sup>4</sup> S. M. Cronenwett, T. H. Oosterkamp, and L. Kouwenhoven, *Science* **281**, 540 (1998).
- <sup>5</sup> R. J. Heary, J. E. Han, and L. Zhu, *Phys. Rev. B* **77**, 115132 (2008).
- <sup>6</sup> K. Ono, D. G. Austing, Y. Tokura, S. Tarucha, *Science* **297**, 1313 (2002).
- <sup>7</sup> A. Vidan, R. M. Westervelt, M. Stopa, M. Hanson, and C. Gossard, *Appl. Phys. Lett.* **85**, 3602 (2004).
- <sup>8</sup> P. Borri, S. Schneider, W. Langbein, U. Woggon, A. E. Zhukov, V. M. Ustinov, N. N. Ledentsov, Z. I. Alferov, D. Ouyang, and D. Bimberg, *Appl. Phys. Lett.* **79**, 2633 (2001); A. V. Uskov, E. P. ÓReilly, M. Laemmlin, N. N. Ledentsov, and D. Bimberg, *Opt. Commun.* **248**, 211 (2005).
- <sup>9</sup> N. N. Ledentsov, V. M. Ustinov, A. Y. Egorov, A. E. Zhukov, M. V. Maksimov, I. G. Tabatadze, and P. S. Kopev, *Semiconductors* **28**, 832 (1994).
- <sup>10</sup> Q. Xie, A. Madhukar, P. Chen, and N. P. Kobayashi, *Phys. Rev. Lett.* **75**, 2542 (1995).
- <sup>11</sup> W. G. van der Wiel, S. De Franceschi, J. M. Elzerman, T. Fujisawa, S. Tarucha, and L. P. Kouwenhoven, *Rev. Mod. Phys.* **75**, 1 (2003).
- <sup>12</sup> N. C. van der Vaart, S. F. Godijn, Y. V. Nazarov, C. J. P. M. Harmans, J. E. Mooij, L. W. Molenkamp, C. T. Foxon, *Phys. Rev. Lett.* **74**, 4702 (1995); F. R. Waugh, M. J. Berry, C. H. Crouch, C. Livermore, D. J. Mar, R. M. Westervelt, K. L. Campman, and A. C. Gossard, *Phys. Rev. B* **53**, 1413 (1996).
- <sup>13</sup> A. W. Holleitner, C. R. Decker, H. Qin, K. Eberl, and R. H. Blick, *Phys. Rev. Lett.* **87**, 256802 (2001).
- <sup>14</sup> M. L. Ladron de Guevara, F. Claro, and P. A. Orellana, *Phys. Rev. B* **67**, 195335 (2003).
- <sup>15</sup> T.-S. Kim and S. Hershfield, *Phys. Rev. B* **63**, 245326 (2001); K. Kang and S. Y. Cho, *J. Phys. Condens. Matter* **16**, 117 (2004).
- <sup>16</sup> K. Kobayashi, H. Aikawa, S. Katsumoto, and Y. Iye, *Phys. Rev. Lett.* **88**, 256806 (2002); *Phys. Rev. B* **68**, 235304 (2003).
- <sup>17</sup> M. Sato, H. Aikawa, K. Kobayashi, S. Katsumoto, and Y. Iye, *Phys. Rev. Lett.* **95**, 066801 (2005); K. Kobayashi, H. Aikawa, A. Sano, S. Katsumoto, and Y. Iye, *Phys. Rev. B* **70**, 035319 (2004).
- <sup>18</sup> D. E. Logan, C. J. Wright, and M. R. Galpin, *Phys. Rev. B* **80**, 125117 (2009); Z. Z. Sun, R. Q. Zhang, W. Fan, and X. R. Wang *J. Appl. Phys.* **105**, 043706 (2009); P. Trocha and J. Barna *Phys. Rev. B* **76**, 165432 (2007); K. Takahashi and T. Aono, *Phys. Rev. B* **74**, 041311 (2006); R. Franco, M. S. Figueira, and E. V. Anda, *Phys. Rev. B* **73**, 195305 (2006).
- <sup>19</sup> V. Moldoveanu, M. olea, A. Aldea, and B. Tanatar, *Phys. Rev. B* **71**, 125338 (2005); Y. S. Joe, A. M. Satanin, and G. Klimeck, *Phys. Rev. B* **72**, 115310 (2005); A. Fuhrer, P. Brusheim, T. Ihn, M. Sigrist, K. Ensslin, W. Wegscheider, and M. Bichler *Phys. Rev. B* **73**, 205326 (2006); T. Kubo, Y. Tokura, T. Hatano, and S. Tarucha, *Phys. Rev. B* **74**, 205310 (2006).
- <sup>20</sup> W. Hofstetter, J. König, and H. Schoeller, *Phys. Rev. Lett.* **87**, 156803 (2001); J. König and Y. Gefen, *Phys. Rev. Lett.* **86**, 3855 (2001); *Phys. Rev. B* **65**, 045316 (2002); B. Kubala and J. König, *Phys. Rev. B* **65**, 245301 (2003).
- <sup>21</sup> K. Kang and S. Y. Cho, *J. Phys.: Condens. Matter* **16**, 117 (2004); H. Lu, R. Lü, and B. F. Zhu, *Phys. Rev. B* **71**, 235320 (2005); Z.-M. Bai, M.-F. Yang, and Y.-C. Chen, *J. Phys.: Condens. Matter* **16**, 4303 (2004).
- <sup>22</sup> M. L. Ladron de Guevara, F. Claro, and P. A. Orellana, *Phys. Rev. B* **67**, 195335 (2003).
- <sup>23</sup> P. Stefański, A. Tagliacozzo, and B. R. Bulka, *Phys. Rev. Lett.* **93**, 186805 (2004); G. H. Ding, C. K. Kim, and K. Nahm, *Phys. Rev. B* **71**, 205313 (2005).
- <sup>24</sup> W. Hofstetter, J. König, and H. Schoeller, *Phys. Rev. Lett.* **87**, 156803 (2001).
- <sup>25</sup> H. Lu, R. Lü, and B. F. Zhu, *J. Phys.: Condens. Matter* **18**, 8961 (2006); H. Lu, R. Lü, and B. F. Zhu, *Phys. Rev. B* **71**, 235320 (2005).
- <sup>26</sup> A. A. Clerk, X. Waintal, and P. W. Brouwer, *Phys. Rev. Lett.* **86**, 4636 (2001).
- <sup>27</sup> Q. F. Sun, J. Wang, and H. Guo, *Phys. Rev. B* **71**, 165310 (2005); Q. F. Sun and X. C. Xie, *Phys. Rev. B* **73**, 235301 (2006).
- <sup>28</sup> F. Chi and S. S. Li, *J. Appl. Phys.* **100**, 113703(2006).
- <sup>29</sup> S. Tanaka, S. Garmon, G. Ordonez, T. Petrosky, *Phys. Rev. B* **76**, 153308 (2007).
- <sup>30</sup> B.H. Wu, J.C. Cao, *J. Phys.: Condens. Matter* **16**, 8285 (2004).
- <sup>31</sup> I. V. Lerner, V. I. Yudson, and I. V. Yurkevich, *Phys. Rev. Lett.* **100**, 256805 (2008).
- <sup>32</sup> L. E. F. Foa Torres, H. M. Pastawski, and E. Medina, *Europhys. Lett.* **73**, 164(2006).
- <sup>33</sup> A. Herzog and U. Weiss, *New J. Phys.* **10**, 045008 (2008); J.-T. Shen and S. Fan, *New J. Phys.* **11**, 113024 (2009).
- <sup>34</sup> S. Jana and A. Chakrabarti, *Phys. Rev. B* **77**, 155310 (2008).
- <sup>35</sup> S. Costamagna and J. A. Riera, *Phys. Rev. B* **77**,

- 235103 (2008).
- <sup>36</sup> B. Jouault, M. Gryglas, M. Baj, A. Cavanna, U. Gennser, G. Faini, and D. K. Maude, *Phys. Rev. B* **79**, 041307(R) (2009).
- <sup>37</sup> V. Vargiamidis and V. Fessatidis, *Phys. Rev. B* **79**, 205309 (2009).
- <sup>38</sup> S. Garmon, H. Nakamura, N. Hatano, and T. Petrosky, *Phys. Rev. B* **80**, 115318 (2009).
- <sup>39</sup> S. Datta, *Electron Transport in Mesoscopic Systems* (Cambridge University Press, Cambridge, England, 1997).
- <sup>40</sup> Y. Meir and N. S. Wingreen, *Phys. Rev. Lett.* **68**, 2512 (1992); A. P. Jauho, N. S. Wingreen, and Y. Meir, *Phys. Rev. B* **50**, 5528 (1994).
- <sup>41</sup> W. Gong, Y. Zheng, Y. Liu, and T. Lü, *Phys. Rev. B* **73**, 245329 (2006).
- <sup>42</sup> Y. Liu, Y. Zheng, W. Gong, and T. Lü, *Phys. Lett. A* **360**, 154 (2006).
- <sup>43</sup> W. Gong, Y. Zheng, Y. Liu, T. Lu, *Physica E* **40**, 618 (2008).
- <sup>44</sup> W. Gong, Y. Han, and G. Wei, *J. Phys.: Condens. Matter* **21**, 175801 (2009).

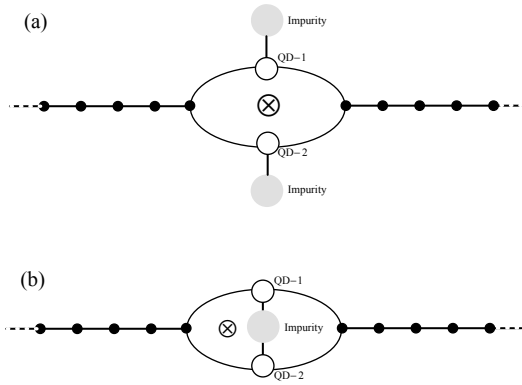


FIG. 1: (a) Schematic of a double QD AB interferometer with a local threading magnetic flux by the presence of impurities.

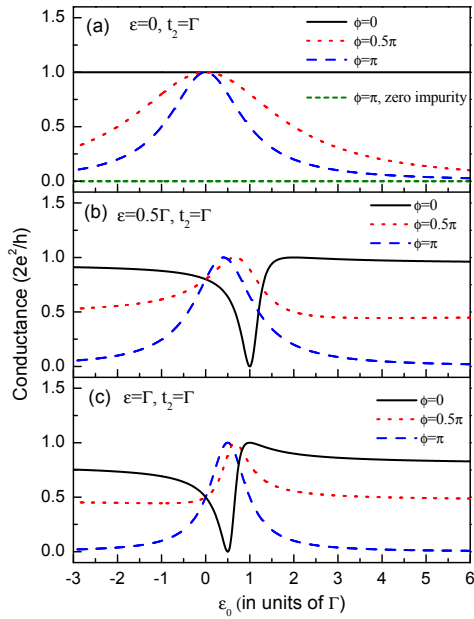


FIG. 2: The conductance spectra affected by the single-level impurity coupled to QD-2. The uniform QD levels are assumed to be 0 in (a),  $0.5\Gamma$  in (b), and  $\Gamma$  in (c).

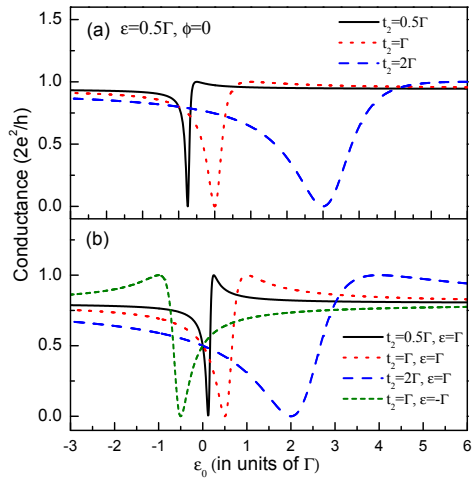


FIG. 3: The spectra of linear conductance with the change of the coupling between QD-2 the impurity.

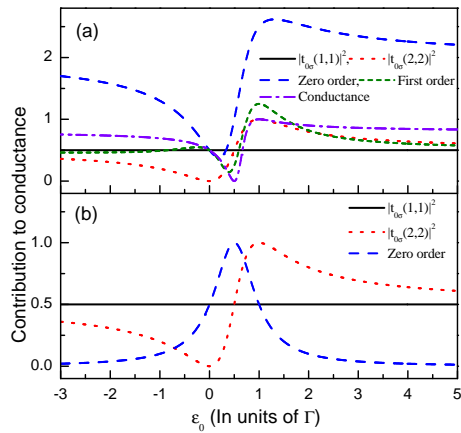


FIG. 4: The Feynman-path analysis of the impurity-modified quantum interference.

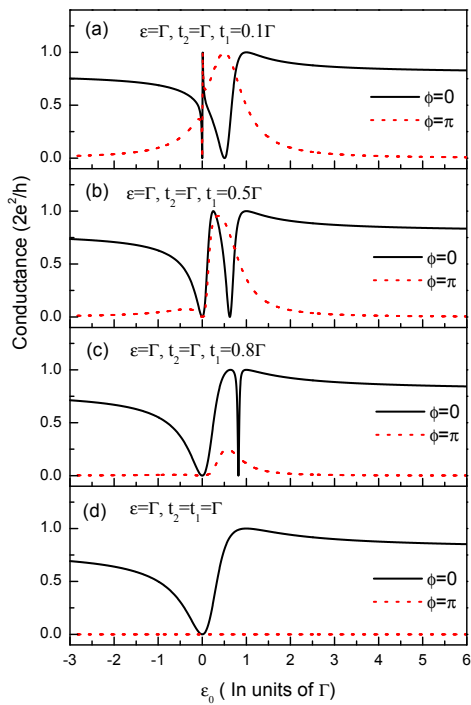


FIG. 5: The conductance curves in the case where each QD couples to a single-level impurity.

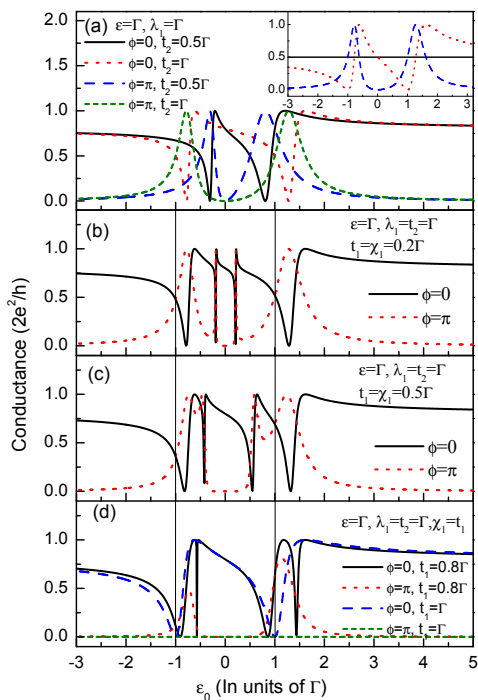


FIG. 6: (a) The conductance spectra in the presence of a double-level impurity side-coupled to QD-2 with the zero-order paths in the inset. (b)-(d) The conductance curves in the case where each QD couples to a double-level impurity.

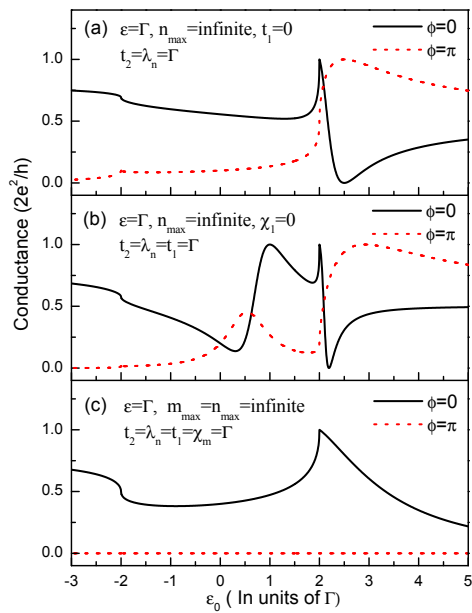


FIG. 7: The linear conductance spectra for the case of infinite-level impurities side-coupled to the QDs of the interferometer.

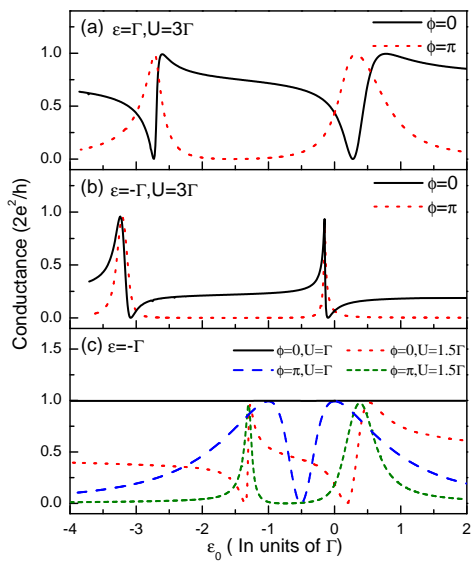


FIG. 8: The impurity-related linear conductance spectra in the case of the many-body terms being considered with  $U = 3\Gamma$  in (a) and (b). In (c),  $U = \Gamma$  and  $1.5\Gamma$ , respectively.

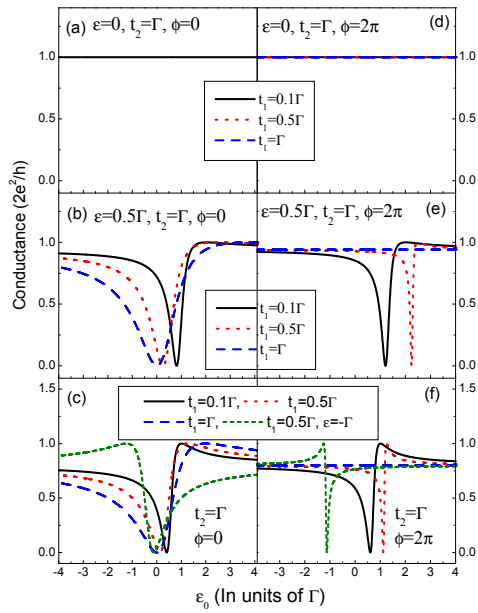


FIG. 9: The conductance curves in the presence of a nonlocal single-level impurity coupled to the QDs, for the cases of  $\phi = 0$  and  $\phi = 2\pi$ .

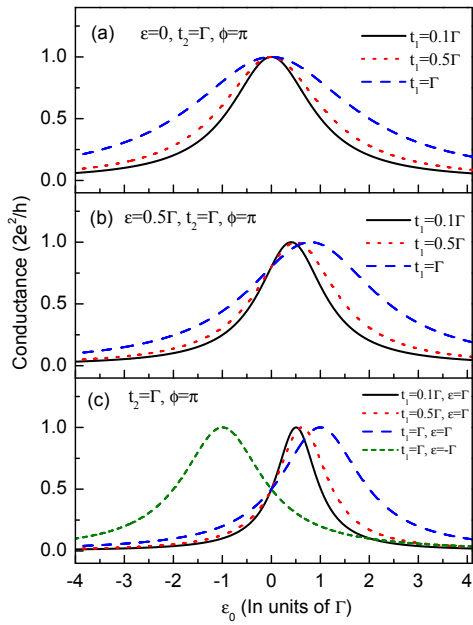


FIG. 10: The conductance curves with a nonlocal single-level impurity coupled to the QDs in the case of  $\phi = \pi$ .

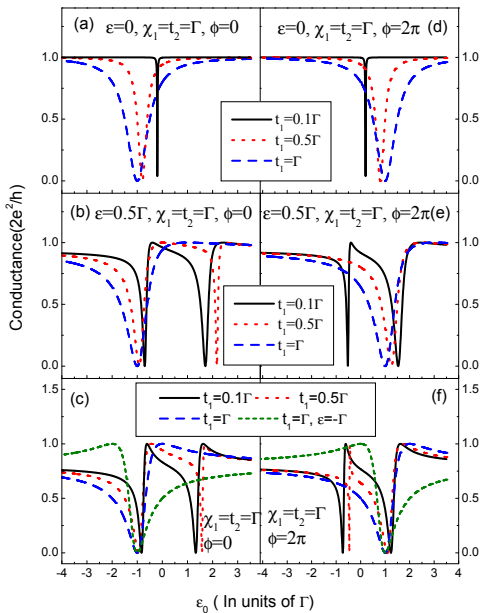


FIG. 11: The conductance curves with a nonlocal double-level impurity coupled to the QDs, for the cases of  $\phi = 0$  and  $\phi = 2\pi$ .

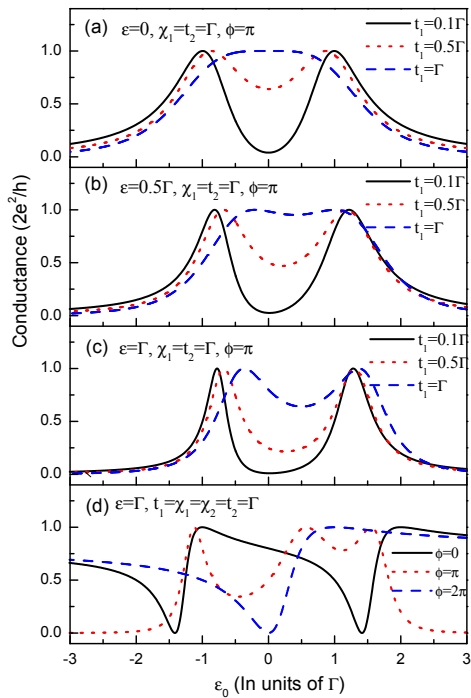


FIG. 12: (a)-(c), the conductance curves with a nonlocal double-level impurity coupled to the QDs when  $\phi = \pi$ . In (d), the spectra about the triple-level nonlocal impurity are shown.

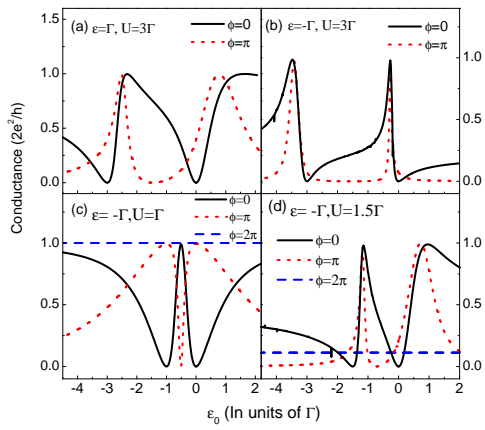


FIG. 13: The nonlocal-impurity-modified linear conductance spectra in the presence of the many-body terms with  $U = 3\Gamma$  in (a) and (b). In (c) and (d),  $U = \Gamma$  and  $1.5\Gamma$  are considered.